



## OPEN ACCESS

## EDITED BY

Susanna Chiocca,  
European Institute of Oncology (IEO), Italy

## REVIEWED BY

Maria Contaldo,  
University of Campania L. Vanvitelli, Italy  
Aidan D. Meade,  
Technological University Dublin, Ireland

## \*CORRESPONDENCE

Tami Yap  
✉ [tspyap@unimelb.edu.au](mailto:tspyap@unimelb.edu.au)

RECEIVED 20 April 2023

ACCEPTED 12 June 2023

PUBLISHED 03 July 2023

## CITATION

Yap T, Tan I, Ramani RS, Bhatia N, Demetrio de Souza Franca P, Angel C, Moore C, Reiner T, Bussau L and McCullough MJ (2023) Acquisition and annotation in high resolution *in vivo* digital biopsy by confocal microscopy for diagnosis in oral precancer and cancer. *Front. Oncol.* 13:1209261. doi: 10.3389/fonc.2023.1209261

## COPYRIGHT

© 2023 Yap, Tan, Ramani, Bhatia, Demetrio de Souza Franca, Angel, Moore, Reiner, Bussau and McCullough. This is an open-access article distributed under the terms of the [Creative Commons Attribution License \(CC BY\)](https://creativecommons.org/licenses/by/4.0/). The use, distribution or reproduction in other forums is permitted, provided the original author(s) and the copyright owner(s) are credited and that the original publication in this journal is cited, in accordance with accepted academic practice. No use, distribution or reproduction is permitted which does not comply with these terms.

# Acquisition and annotation in high resolution *in vivo* digital biopsy by confocal microscopy for diagnosis in oral precancer and cancer

Tami Yap<sup>1,2\*</sup>, Ivy Tan<sup>1,2</sup>, Rishi S. Ramani<sup>1</sup>, Nirav Bhatia<sup>2</sup>, Paula Demetrio de Souza Franca<sup>3,4</sup>, Chris Angel<sup>5</sup>, Caroline Moore<sup>1</sup>, Thomas Reiner<sup>3</sup>, Lindsay Bussau<sup>6</sup> and Michael J. McCullough<sup>1,2</sup>

<sup>1</sup>Melbourne Dental School, Faculty of Medicine, Dentistry and Health Sciences, Carlton, VIC, Australia, <sup>2</sup>Oral Medicine Unit, Royal Dental Hospital of Melbourne, Carlton, VIC, Australia, <sup>3</sup>Department of Radiology, Memorial Sloan Kettering Cancer Center, New York, NY, United States, <sup>4</sup>Department of Otorhinolaryngology and Head and Neck Surgery, Federal University of São Paulo, São Paulo, SP, Brazil, <sup>5</sup>Department of Pathology, Peter MacCallum Cancer Centre, Victorian Comprehensive Cancer Centre, Parkville, VIC, Australia, <sup>6</sup>Optiscan Imaging, Mulgrave, VIC, Australia

**Introduction:** Scanned fibre endomicroscopes are full point-scanning confocal microscopes with submicron lateral resolution with an optical slice thickness thin enough to isolate individual cell layers, allow active positioning of the optical slice in the z-axis and collection of megapixel images. Here we present descriptive findings and a brief atlas of an acquisition and annotation protocol high resolution *in vivo* capture of oral mucosal pathology including oral squamous cell carcinoma and dysplasia using a fluorescence scanned fibre endomicroscope with 3 topical fluorescent imaging agents: fluorescein, acriflavine and PARPi-FL.

**Methods:** Digital biopsy was successfully performed *via* an acquisition protocol in seventy-one patients presenting for investigation of oral mucosal abnormalities using a miniaturized, handheld scanned fibre endoscope. Multiple imaging agents were utilized and multiple time points sampled. Fifty-nine patients had a matched histopathology correlating in location with imaging. The images were annotated back to macrographic location using a purpose-built software, MouthMap™.

**Results:** Acquisition and annotation of cellular level resolved images was demonstrated with all 3 topical agents. Descriptive observations between clinically or histologically normal oral mucosa showed regular intranuclear distance, a regular nuclear profile and fluorescent homogeneity. This was dependent on the intraoral location and type of epithelium being observed. Key features of malignancy were a loss of intranuclear distance, disordered nuclear clustering and irregular nuclear fluorescence intensity and size. Perinuclear fluorescent granules were seen in the absence of irregular nuclear features in lichenoid inflammation.

**Discussion:** High resolution oral biopsy allows for painless and rapid capture of multiple mucosal sites, resulting in more data points to increase diagnostic precision. High resolution digital micrographs can be easily compared serially across multiple time points utilizing an annotation software. In the present study we have demonstrated realization of a high-resolution digital biopsy protocol of the oral mucosa for utility in the diagnosis of oral cancer and precancer..

#### KEYWORDS

oral cancer, confocal, endomicroscope, OSCC (oral squamous cell carcinoma), dysplasia, fluorescence, oral potentially malignancy disorders (OPMDs), digital health

## 1 Introduction

Despite the current global trend in tobacco reduction, oral squamous cell carcinoma (OSCC) is still an important health concern. Individuals diagnosed at advanced stages undergo extensive surgery and postoperative adjuvant therapies with resultant impact on quality of life. Furthermore, patients with late stage OSCC experience a poorer 5-year disease-survival rate of 40.7%. However, with early stage diagnosis, prognosis has a much higher five-year survival rate, reaching over 84% (1). Therefore, timely detection plays a crucial role in improving the survival rates and post-treatment quality of life for patients with OSCC.

The diagnosis of OSCC at an early stage requires using a combination of conventional expert oral examination and scalpel biopsy (2). Oral potentially malignant disorders (OPMDs) are visible changes of the oral mucosa that are associated with transformation into and increased risk of OSCC that affect up to 5% of the general population (3). The most common OPMDs are oral leukoplakia, oral lichen planus (OLP), and oral lichenoid lesions (OLL) with an overall malignant transformation rate varying from 1.1 to 4.3% (4, 5). Although screening for OPMDs increases the chance of early stage diagnosis (6), there currently remains limited capacity for prediction of the development of malignancy in any one individual and for any particular oral lesion. Diagnostic challenges include the lack of uniform progression rates (ranging from 6%–36%) and variable association with degrees of dysplasia in OPMDs.

Invasive intraoral biopsies are typically performed under local anesthetic in an outpatient setting. These procedures cause anxiety in patients, resulting in subsequent oral post-procedural pain. Further, histopathological conclusions made on the tissue sample excised are presumptively applied to the remainder of abnormal mucosa. Non-invasive tools that aim to provide cellular level resolved, rapid, multisite insight beyond white light visualization of the oral mucosa is being continually developed.

Here we use high-resolution fluorescence confocal microscopy with 3 different topical fluorescence agents to address this clinical need. Confocal microscopy is an optical imaging technique that increases optical resolution and contrast of a micrograph by means of adding a spatial pinhole placed at the confocal plane of the lens to eliminate out-of-focus light (7). It allows for real-time, non-

invasive, microscopic field of view assessment of material of interest.

Confocal microscopes may utilize reflectance or fluorescence imaging, or both (8). The structural visualization of reflectance confocal microscopy is dependent on the refractive index differences in the tissue and doesn't require introduction of a fluorophore into the tissue. Thereby, it is not limited by fluorescence latency (9). Reflectance confocal microscopy has been explored in diagnosis of oral mucosal disease including oral dysplasia, oral lichen planus and cancer extensively by Contaldo et al. (10, 11) Fluorescence confocal microscopy requires introduction of a fluorophore into the tissue that allows for targeting of specific structures, which may preferentially bind the fluorophore allowing for targeted visualization. However, miniaturization of capturing probe to be introduced in the oral cavity is an important consideration when using confocal microscopes in assessing oral mucosal disease. Another acquisition consideration is the mobility of *in vivo* oral tissues and the presence of saliva in a patient who is seen in an outpatient setting without sedation or general anesthesia.

Highly miniaturized handheld confocal microscopes for use *in vivo* have been developed, and these are known as endomicroscopes. There are 2 types of endomicroscope - scanned fibre and bundle fibre devices. The most important difference between the 2 technologies in the fundamental context of cancer diagnosis is resolution. The imaging resolution of bundle fibre devices is limited by the number of fibres in the bundle, the fixed z-focus-depth and the thick z-section collected by the device. Only one focal point per fiber can be collected, thus limiting the resolution. Typically, bundle fibre devices cannot resolve cells and subcellular features required for diagnostic assessment (12). Differently, scanned fibre endomicroscopes are full point-scanning confocal microscopes with submicron lateral resolution and an optical slice thickness thin enough to isolate individual cell layers, active positioning of the optical slice in the z-axis and collection of megapixel images. What this means is that scanned fibre endomicroscopes collect images with cellular and subcellular resolution enabling assessment of histological features in real-time *in vivo* images. Scanned fibre confocal microscopy has been used for *in vivo* identification of cancer, precancer and other diseases of the mouth, esophagus, cervix, colon and brain (13–19).

Employed topical fluorescent contrast dyes used for epithelial architecture visualization in mucosal studies includes acriflavine, a

common topical antiseptic, and fluorescein, an exogenous dye used routinely in ophthalmic practice for detection of foreign bodies and corneal abrasions (20, 21). Fluorescein and acriflavine can be considered pancytoprotopheral fluorescent agents as they non-selectively bind membrane and nuclear material, regardless of molecular activity. Acriflavine has been used in combination with several types of confocal microscope technology, including point scanning to visualize and diagnose oral mucosal disease (18, 22). PARP1 (Poly (ADP-ribose) polymerase 1 is a nuclear protein that has been found to be overexpressed in many malignancies including ovarian cancer, breast cancer and OSCC (23). Reiner et al. first reported the small molecule PARPi-FL, a fluorescent dye-based imaging agent, that binds to PARP1 (24). PARPi-FL is based on the PARP1 inhibitor olaparib (Lynparza) that is FDA-approved for the treatment of several types of cancer, but mostly used for the treatment of ovarian cancer. PARPi-FL is intended as an indicator of PARP1 activity and has been shown to delineate tumor detection from normal tissue in mice models, *ex vivo* human tissue (25), and *in vivo* in a Phase I clinical trial as a mouthwash (26). PARPi-FL can be used as a molecule-specific fluorescence agent.

Another important consideration with cellular level imaging is reference back to the mucosal site from which the image was captured. Further, to allow multiple time points or locations to be easily and practically compared, an annotation tool to map the mouth is needed.

The aims of the present study were to

- validate the use of a scanned fibre endomicroscope protocol to perform non-invasive, real-time high resolution digital biopsy of the oral mucosa.
- present a brief image atlas that documents the comparative features of *in vivo* microscopy of histopathology-diagnosed oral mucosal conditions.
- demonstrate the use of 3 different topical fluorophores in acquiring cellular level resolved images.

## 2 Material and methods

This exploratory, phase I, single-center, open-label, prospective Privacy Act of 1988 compliant study was approved by the University of Melbourne Medicine and Dentistry Human Ethics Sub-Committee (ID 1955205) and conducted in accordance with the Declaration of Helsinki. Written informed consent was obtained from all patients.

### 2.1 Participants

Patients were consecutively recruited from the Oral Medicine Department of the Royal Dental Hospital Melbourne. Individuals attending for assessment of oral mucosal abnormalities, including

OPMDs or with a history of oral cancer were invited to participate.

### 2.2 Synthesis of PARPi-FL

PARPi-FL was produced by our collaborators at Memorial Sloan Kettering (MSK) Cancer Center in New York, USA, as previously described (27), and fast shipped to Australia in dry ice. Briefly, triethylamine (NEt<sub>3</sub>) >99.5% purity, Trifluoroacetic acid (TFA) ReagentPlus 99%, and dimethyl sulfoxide-d<sub>6</sub> (DMSO-d<sub>6</sub>) were purchased from Sigma-Aldrich (St. Louis, MO). Anhydrous acetonitrile (CH<sub>3</sub>CN) over molecular sieve, HPLC-grade acetonitrile, BODIPY FL NHS ester, and Texwipe Technicloth were purchased from Thermo Fisher Scientific (Waltham, MA). Water (18.2 MΩ cm<sup>-1</sup> at 25 °C) was obtained from an Alpha-Q Ultrapure water filtration system from Millipore (Bedford, MA). PARP-NH precursor (4-(4-fluoro-3-(piperazine-1-carbonyl)benzyl)phthalazin-1(2H)-one) was synthesized at MSK according to protocols reported earlier. PARPi-FL was produced under good manufacturing practice (GMP) conditions at MSK under IND number 133,109. Briefly, BODIPY-FL NHS ester (5.0 mg, 12.8 μmol, 1.0 eq.) was conjugated to 4-(4-fluoro-3-(piperazine-1-carbonyl) benzyl) phthalazin-1(2H)-one (9.4 mg, 25.6 μmol, 2.0 eq.) in the presence of Et<sub>3</sub>N (6.3 μL) in anhydrous acetonitrile for 4 h at room temperature. Purification by preparative HPLC (Phenomenex Jupiter 5u C18 300A, 10 × 250 mm, 3 mL/min, 5 to 95% of acetonitrile (0.1% TFA) in 15 min) and subsequent lyophilization yielded PARPi-FL (5.9 mg, 73%) as a red solid. Analytical HPLC analysis (Waters' Atlantis T3 C18 5 μm, 4.6 × 250 mm, 3 mL/min, 5 to 95% of acetonitrile (0.1% TFA) in 15 min) showed high purity (99.27%, *t<sub>R</sub>* = 14.2 min) of the imaging agent. The identity of PARPi-FL was confirmed using LC-MS (MS (+) *m/z* = 621.15 [M-F]<sup>+</sup>) and NMR (consistent with structure).

### 2.3 Confocal microscope

The InVivage® (Optiscan Imaging, Victoria Australia) system at the time of this study was an investigational medical device for the purposes of this study only. The system has a software interface which allows for adjustment of laser power, depth, refresh rate, capture methods and macro data which is connected to the image output which can be selected to map back based on the chosen intraoral location (Figure 1). Briefly, the InVivage® system is a hand-held scanned fibre confocal endomicroscope that acquires images using a single channel for illumination and detection of 488 nm excitation, with a lens NA of 0.3 (similar to a 10 × objective) and a field of view of 475 μm × 475 μm. The resolution capabilities are 0.55 μm lateral and 5.1 μm axial. The system is used by placing the probe in direct contact with the tissue, after treatment with a dye, to acquire images at different depths along the Z axis (28). The physical image plane can be translated from the surface to 400 μm but imaging depth with topical application was typically from

tissue surface to a depth of 100  $\mu\text{m}$ . Further setting details are described below under Image Acquisition.

## 2.4 Clinical protocol

The clinical protocol was as follows:

- 1) Oral cavity examination performed by an oral medicine specialist that included a systematic inspection of all mucosal surfaces.
- 2) Registration of all intraoral lesions by macrographic photography (Canon EOS 200D Canon 100mm F2.8 Macro USM)
- 3) Confocal microscope imaging (InVivage®). The patients were imaged with a single or multiple agents in the following order:
  - a. *PARPi-FL* Patients were instructed to swish a 10 mL solution of 1 $\mu\text{M}$  PARPi-FL in 30% PEG 300 and 70% water for 1 minute, followed by a 30-second water rinse, and then undergo digital microscopic fluorescence imaging.
  - b. *Fluorescein* - Patients were asked to swish 10 mL of a 0.1% solution of fluorescein in sterile water for 1 minute, followed by a water rinse that was repeated until the rinsed water appeared clear. Then, they underwent digital microscopic fluorescence imaging.
  - c. *Acriflavine* - Mucosal areas of interest were painted with a cotton swab soaked in a solution of 0.1% acriflavine in sterile water, followed by a 1-minute water rinse that was

repeated until the rinsed water appeared clear. Digital microscopic fluorescence imaging was then performed.

## 2.5 Image acquisition

Image location-site selection was dependent on the intraoral location of mucosal abnormality. The terms are defined as follows: image location was defined as one of 20 intraoral areas which together captured all areas of the oral cavity by macrographic photography and was compatible with the mapping software we developed called MouthMap™ (Figures 2, 3). Image site was defined as the specific point at which the probe was placed when the image capture occurred. An image set was defined as a set of images acquired using a single fluorescence agent collated by location and sites.

The control location-sites were completed at the buccal mucosa and/or the contralateral surface if clinically normal oral mucosa was present. Capture at an image site was made by placing the probe on the site of interest and capturing a Z-stack. The Z-stack image acquisition commences at the surface of the probe into the tissue until the depth of 100 $\mu\text{m}$  with 5  $\mu\text{m}$  incremental focal plane advancements. This Z-stack command occurred utilizing a programmed single foot pedal command (Figure 2) so that the user could remain otherwise immobile whilst supporting the intraoral tissues. For all patient imaging, we used long pass filter of 515– 815 nm, and a scanning speed of 1024 pixels x 512 lines with a frame rate of 0.7 seconds per frame. The settings of the laser power are set at 100%, when imaging with PARPi-FL, and between 10-25% when imaging with fluorescein and acriflavine.

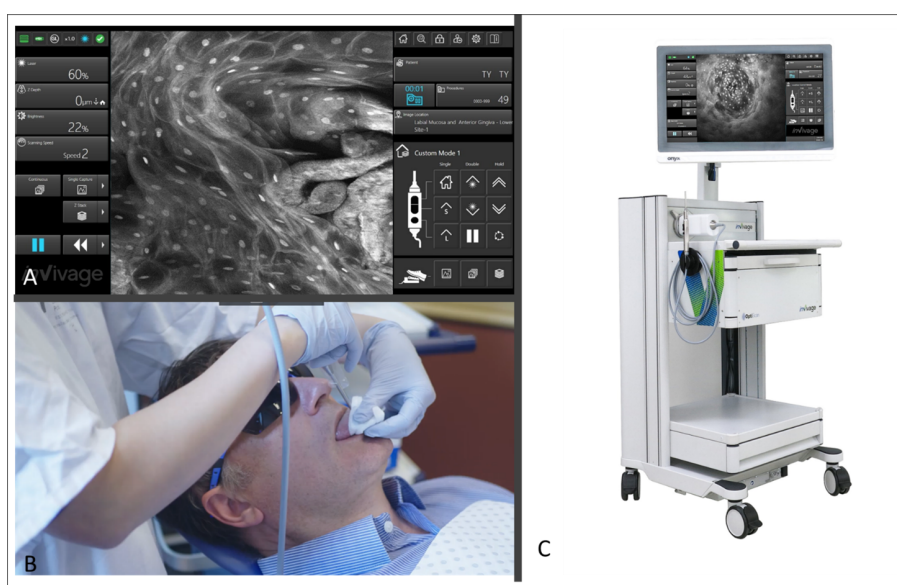


FIGURE 1

(A) Software interface of the InVivage® demonstrating laser and capture settings on the left-hand side and location and patient selection on the right-hand side panel (B) Handheld intraoral probe and command handpiece allows the user to adjust settings without de-gloving (C) The portable InVivage® unit can be transported alongside a conventional dental chair.

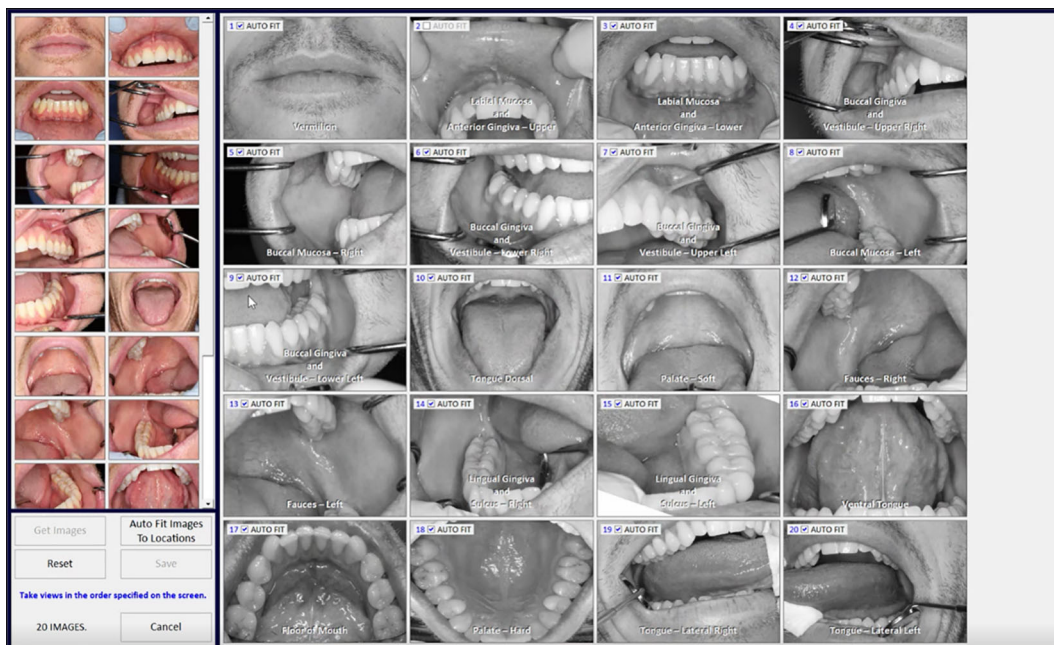


FIGURE 2 MouthMap™ interface showing macrographs allocated into the 20 intraoral locations.

## 2.6 Location annotation

We developed a custom-made software, MouthMap™ which was used to map micrographs captured with the InVivage® and paired with software-housed macrographs classified under 20 intraoral locations (Figure 2). Location and site linkage used the macro data captured on the micrograph Dicom files which link back to the macroscopic intraoral location. Sites were annotated on the

macrographs and the micrographic images were linked and uploaded for visualization (Figure 3).

## 2.7 Diagnosis

Standard of care scalpel biopsy and diagnosis by histopathology was completed at the discretion of the attending clinician. Indication

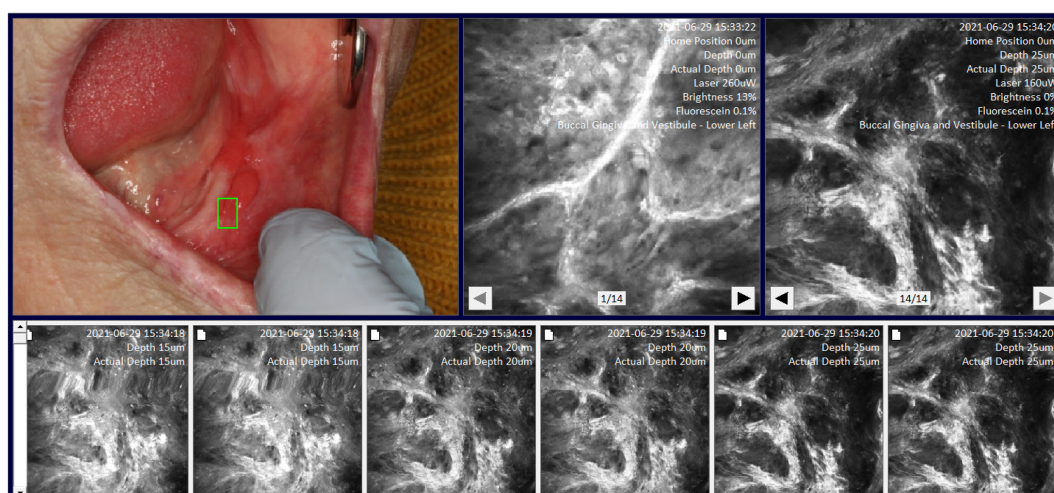


FIGURE 3 Site specific micrographs of the right lateral surface of the tongue visualized in MouthMap™ demonstrating time stamp, location, and laser setting image macros. Image captures are 475µm (W) x 475µm (H).

for prospective biopsy included if histopathology was required for definitive diagnosis of a new or changed clinical presentation. Selection of biopsy site was selected as per standard care and before applying the confocal microscope.

## 2.8 Longitudinal capture

Participants were reapointed for review of their oral lesions as per standard of care. During the review periods, these individuals may have undergone medical therapy, excision of their lesions or regular monitoring.

## 2.9 Data management

Clinical data was collected under a deidentified research ID and managed using REDCap electronic data capture tools hosted at the University of Melbourne (29, 30).

## 3 Results

### 3.1 Patient cohort

Seventy-one patients were recruited for this project, including 33 women and 38 men (43.5% and 53.5% respectively) with a mean age of  $64 \pm 12.2$  years old (range 32 - 88 years). Patients were seen and imaged 1 to 5 times during the study period. Fifty-four (76.0%) of patients presented with a keratotic and/or erythematous mucosal

abnormality of the oral cavity mucosa. Histological correlation was obtained from 83% ( $n = 59$ ) of the imaged patients (Table 1). Histopathological diagnostic categories included hyperkeratosis or hyperplasia, no dysplasia, dysplasia, oral lichenoid inflammation, or oral squamous cell carcinoma. Out of the 12 patients that did not have a histopathological correlation, 8 patients' cases being followed up for oral lichen planus or oral lichenoid lesions diagnosed with a previous biopsy (prior to the inclusion in this protocol) and 4 patients had a clinical diagnosis of either benign alveolar ridge keratosis ( $n=2$ ), post-excision scar ( $n=1$ ) or traumatic ulceration ( $n= 1$ ).

### 3.2 Types of imaging agents

A total of 307 imaging sets were captured which included 109 using PARPi-FL, 93 using fluorescein and 105 using acriflavine. Successful imaging acquisition with cellular level resolution was achieved with all 3 imaging agents: PARPi-FL, acriflavine and fluorescein using the described protocol. PARPi-FL was utilized as a molecule-targeted fluorescence agent. It was expected to bind to less nuclear material than the pancytoarchitectural dyes, and therefore have less signal flooding. The majority of imaged lesions did not have nuclear PARPi-FL pickup. Some non-specific, non-nuclear PARPi-FL signal was observed in highly keratinized lesions similar to that found with acriflavine and fluorescein. The fluorescein stain provided better visualization of cell membranes, whereas the acriflavine stain provided better nuclear visualization (Figures 4A–C).

### 3.3 Intraoral regional mucosal variation

Observations of clinically normal oral mucosa show generally regular intranuclear distance between the keratinocyte cells, a regular cellular outline, and a regular nuclear profile. A typical regular nuclear profile consists of homogenous nuclear fluorescence and size. However, there was an observable microscopic variation in the visualization of clinically normal oral mucosa. This was dependent on the location and type of epithelium being observed. These variations differed depending on if the mucosa is keratinized vs non keratinized, or in an area where a microbial plaque was expected, such as the gingiva (Figure 5). Microbial presence was also observed (Figure 6).

### 3.4 Oral squamous cell carcinoma

There were obvious and striking visual differences between micrographs captured of normal mucosa and OSCC (Figures 7, 8). Key features in micrographs demonstrating malignancy with both fluorescein and acriflavine were a loss of intranuclear distance, disordered nuclear clustering and irregular nuclear fluorescence

TABLE 1 Histopathological conclusion of 59 micrograph matched biopsies.

Histopathological Conclusion	(n of 59)
squamous cell carcinoma	3
high grade dysplasia	5
low grade dysplasia	7
atypia insufficient for dysplasia	2
verrucous hyperplasia	2
hyperkeratosis and or hyperplasia	17
consistent with OLP or lichenoid inflammation	13
<b>Other:</b>	
amalgam tattoo	1
chronic inflammation	2
denture associated gingival hyperplasia	2
fibroepithelial polyp	2
papilloma or focal papillomatosis	2
verruciform xanthoma	1

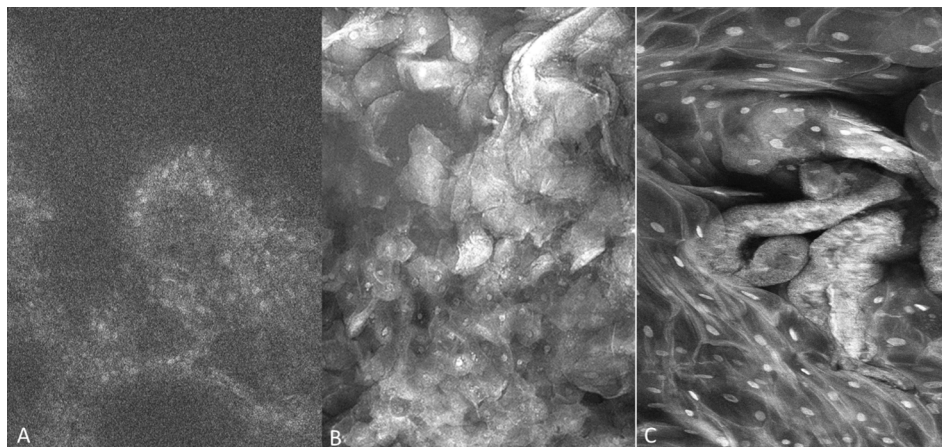


FIGURE 4

Fluorescence images capture with molecule-targeted 1 $\mu$ M topical PARPi-FL (A) and pan-cytoarchitectural fluorescent agents topical 0.1% fluorescein (B) and 0.1% acriflavine (C). Images are 335 $\mu$ m (W) x 475 $\mu$ m (H).

intensity and size. There was a loss of cellular outline and definition, with the nuclei appearing globular, crowded and or clumped visually.

### 3.5 Oral dysplasia

Visual changes seen in low-grade oral dysplasia possess some shared changes with OSCC but are less overt. These include a subtle and progressive dishomogeneity in nuclear size, fluorescence, and inconsistent loss intranuclear distance. Cellular outline is often still visibly appreciated (Figure 9). Nonspecific PARPi-FL binding was seen in highly keratinized areas. PARPi-FL nuclear binding was also seen in low-grade dysplasia with demonstration of retained

intranuclear distance (Figures 10, 11). High grade dysplasia looked similar if not indistinguishable from OSCC (Figure 11).

### 3.6 Hyperkeratosis and hyperplasia

In the presence of hyperkeratosis, it was important to assess the cellular outline regularity as nuclei were not always observable (Figure 12). Secondly, it is imperative to note if there was a vertical component such as benign and malignant exophytic lesions because the confocal probe placement will invariably flatten the tissue, thereby influencing the presentation. Benign hyperkeratosis and hyperplasia could present with an appearance of pseudo-loss of

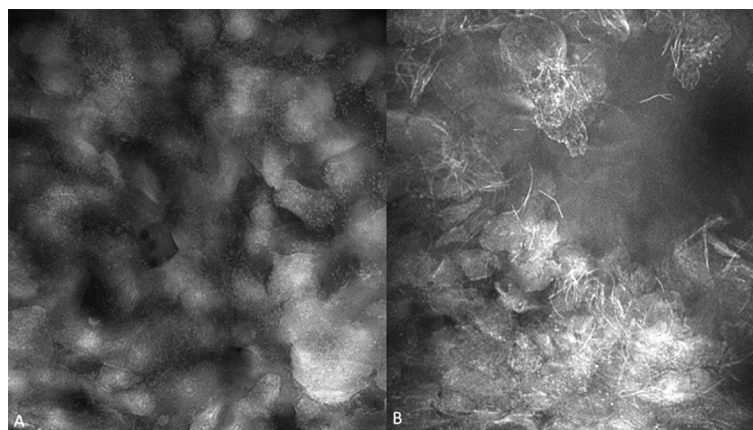
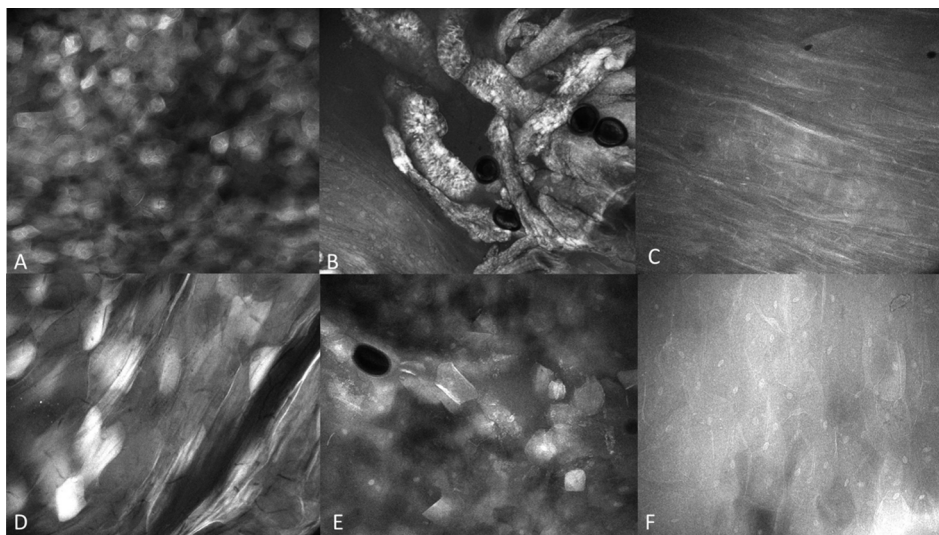


FIGURE 5

(A) Bacterial plaque and pellicle debris visualized on the gingiva; (B) Candidal hyphae observed in verrucous hyperplasia of the buccal mucosa with 0.1% fluorescein. Images are 422  $\mu$ m (W) x 400 $\mu$ m (H).



**FIGURE 6** Regional mucosal variation with the InVivage® utilizing topical 0.1% fluorescein (A) keratinized epithelium of the hard palate, (B) specialized epithelium with papillae of the dorsal tongue, (C) transitional epithelium of the lateral tongue, (D) non-keratinized epithelium of the soft palate, (E) gingival epithelium, (F) buccal mucosa with fluorescein. Images are 475µm (W) x 400µm (H).

internuclear distance, however the regular dimensions of both the cellular and nuclear profile remains intact (Figure 13).

fluorescence was not infrequently observed in other diagnoses along with the features described above.

### 3.7 Oral lichenoid inflammation

The epithelium observed with oral lichenoid inflammation demonstrated regular nuclear size, fluorescence, spacing as well as cellular outline including with prominent and widespread perinuclear fluorescent granules (Figure 14). Perinuclear granular

### 4 Discussion

Patients with OPMDs often have multiple lesions that can cover large areas within the oral cavity. Repeat biopsies of those lesions can cause a significant reduction in quality of life for the patient from both a functional and cosmetic perspective. High resolution *in*

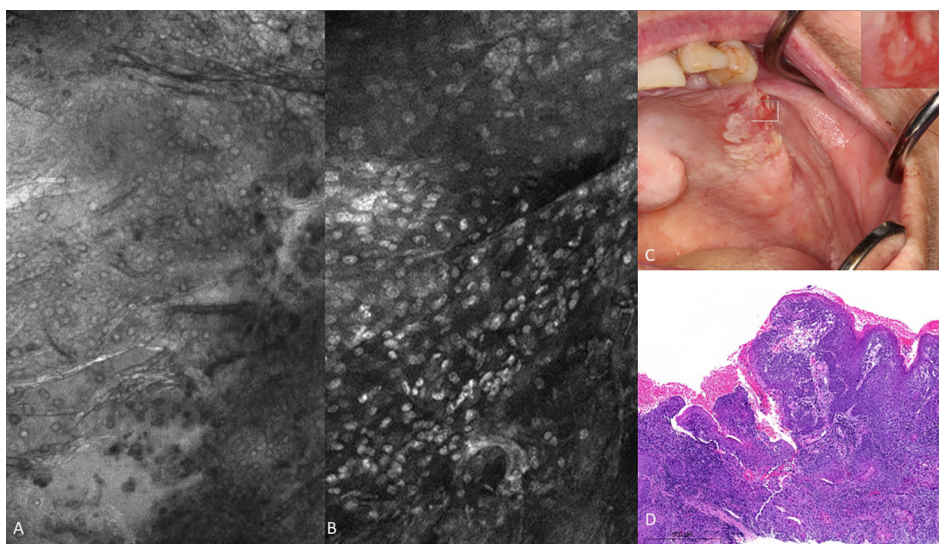


**FIGURE 7** Oral squamous cell carcinoma of the left edentulous maxillary alveolus (A) Micrograph using topical 0.1% fluorescein [282µm (W) x 475µm (H)], (B) Micrograph using 0.1% acriflavine [282µm (W) x 475µm (H)], (C) Digital macrograph of red and white lesion on left maxillary alveolus, inset upper right corner is enlargement of area using magnifying visual tool in MouthMap™ (D) H&E-stained histopathology (500µms scale bar).



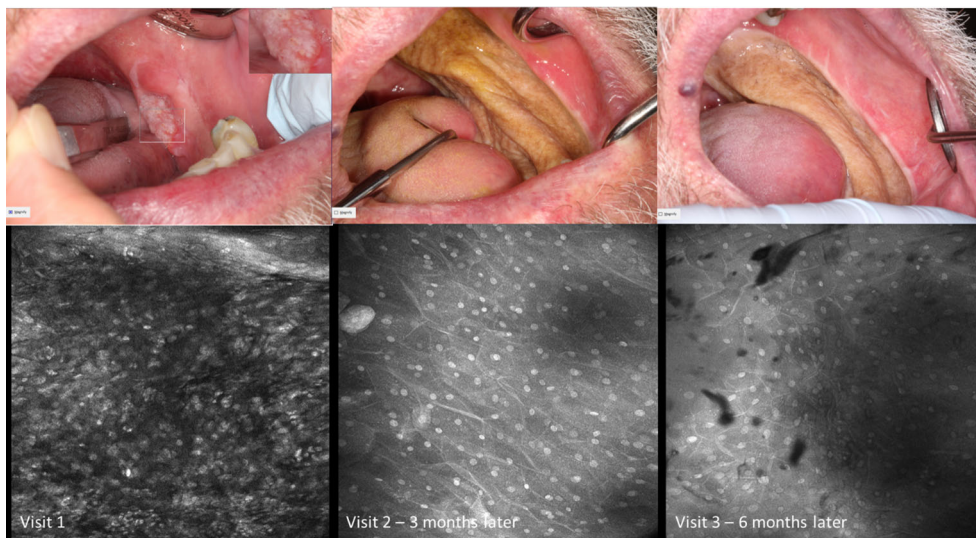


**FIGURE 8** Micrography over time with topical 0.1% acriflavine demonstrating oral squamous cell carcinoma at Visit 1 and subsequent clinically normal non-keratinized mucosa adjacent to radial forearm free flap following resection. Images are 475µm (W) x 475µm (H).

*in vivo* microscopic assessment of the squamous epithelial oral mucosa allows simultaneous assessment of multiple lesions within the oral cavity. These micrograph images allow for serial comparison during subsequent confocal examinations, thus enabling analysis of tissue changes over time precluding the potential need for further biopsies.

In the present study we have performed digital biopsies of the mouth with a high resolution microscopic *in-vivo* visualization of the oral mucosa using 3 topical fluorescence agents using a protocol reproduced in over 300 imaging sets. We have demonstrated micrographs captured with the InVivage® scanned fibre device within an individual oral cavity over time. Our findings further

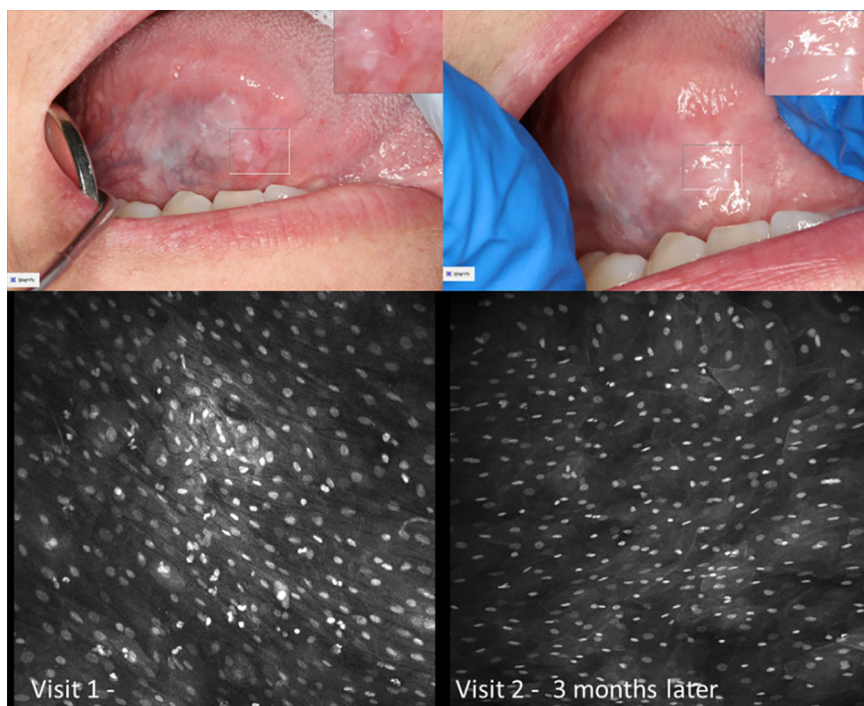


**FIGURE 9** Macroscopic and micrographic images with topical 0.1% acriflavine demonstrating mild dysplasia over time. Macroscopic photos, with right upper corner magnification viewed in MouthMap™, taken pre scalpel biopsy which was performed at Visit 1. Micrographically, the cellular outline and a regular intranuclear distance can be observed despite variability in nuclear size and fluorescence intensity. Images are 475µm (W) x 475µm (H).

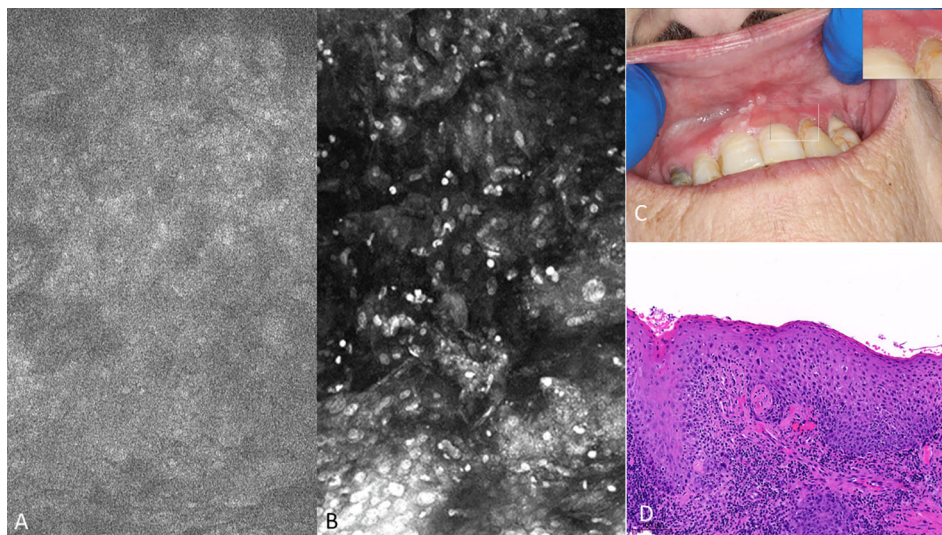


**FIGURE 10**  
Mild dysplasia of the gingiva between the upper left central and lateral incisor (A) visualized with 1 $\mu$ M topical PARPi-FL demonstrating positive nuclei [275 $\mu$ m (W) x 475 $\mu$ m (H)] (B) visualized with topical 0.1% acriflavine [275 $\mu$ m (W) x 475 $\mu$ m (H)] (C) macrographic photo with right upper corner magnification views in MouthMap™ and (D) H&E histopathology (100  $\mu$ m scale bar).

advance understanding of the variation present in the *in vivo* microscopic landscape of abnormal oral mucosa in a novel way (31). Our findings build on work in the field which we recently summarized (32), including exploration with reflectance microscopy, fibre bundle, scanning mirror and precursor scanning fibre technology. Advancements in confocal microscopy proceed on the fronts of probe miniaturization, increased resolution and fluorescence targeting.

The proposed device and the feature of InVivage® System’s ability to detect only in-focus light provides a micro-anatomical cellular level that exceeds the resolution of currently available

devices used for screening and surgical microscopes. We have demonstrated the utility of 3 fluorescent agents to acquire images with cellular level resolution.

One of the limitations of this workflow is that the agents are introduced topically. Whilst this is non-invasive and acceptable for the patient, the depth of penetration of the dyes determines the depth of visualization. For example, assessment could not be made regarding the connective tissue epithelium interdigitation or disruption or blood vessels within the connective tissue. This was the likely reason why severe dysplasia could not be differentiated from OSCC.

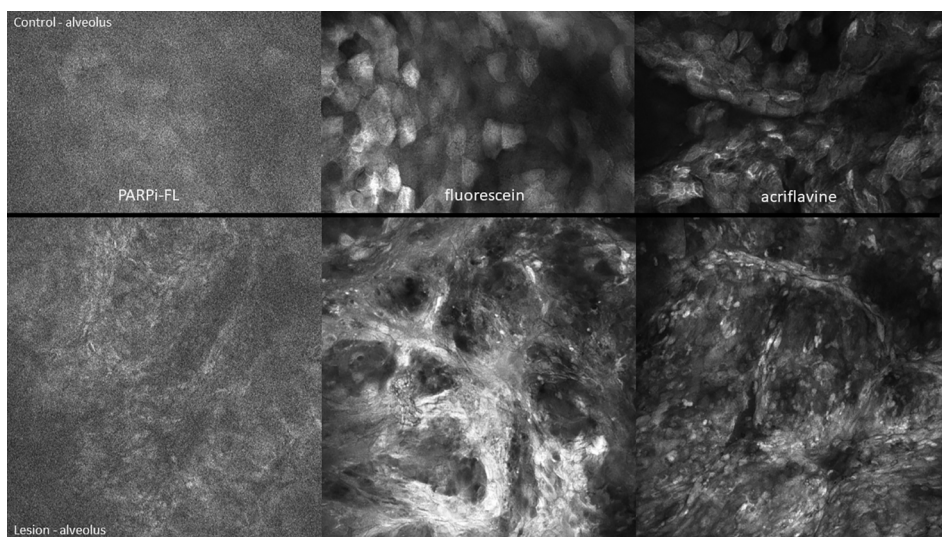


**FIGURE 11**  
High-grade dysplasia of the lower left alveolus [lower panels 475 $\mu$ m (W) x 475 $\mu$ m (H)] and the contralateral clinically normal appearing mucosa [upper panels 475 $\mu$ m (W) x 300 $\mu$ m (H)]. Visualized using topical 1 $\mu$ M PARPi-FL, 0.1% fluorescein and 0.1% acriflavine.

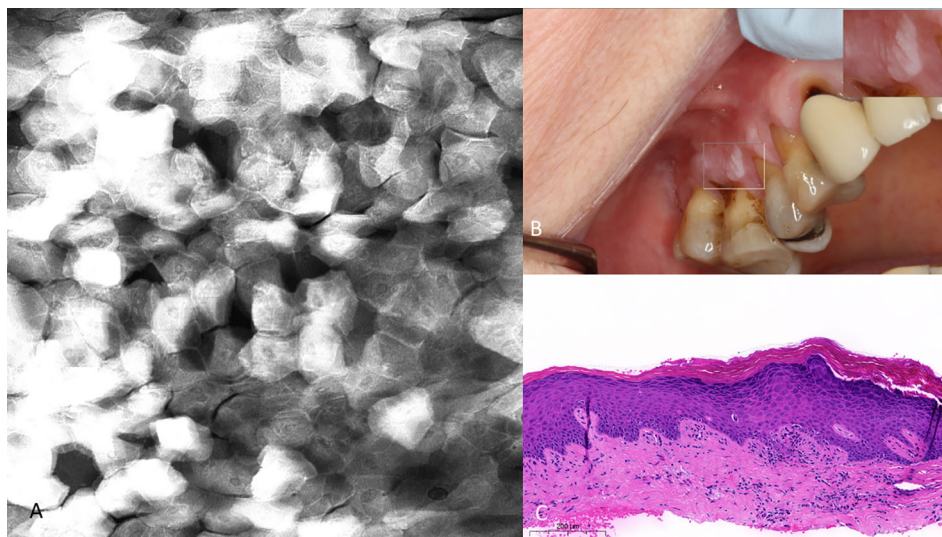


**FIGURE 12**  
**(A)** Hyperkeratosis of the upper right gingiva (clinically non-dysplastic leukoplakia) with 0.1% topical fluorescein 475µm (W) x 475µm (H). Note the regularity of cellular dimensions despite variable fluorescent signal intensities. **(B)** Macrograph photo with right upper corner magnification views in MouthMap™. **(C)** H&E slide (scale bar 200µm).

Exploration with PARPi-FL in visualizing OPMDs was important, but its application is likely of a higher clinical value in patients with a known diagnosis of OSCC where the extension of the lesion is the query. In patients with OSCC, the presence of known neoplasia allows determination of an accurate focal depth to

survey the mucosa. Without this positive visualization reference, it is a challenge to determine where you are located within the mucosa to visualize non-neoplastic oral mucosa. This supports a call for the use of simultaneous 2-channel detection, and development and testing of new or modified fluorescent agents emitting light in

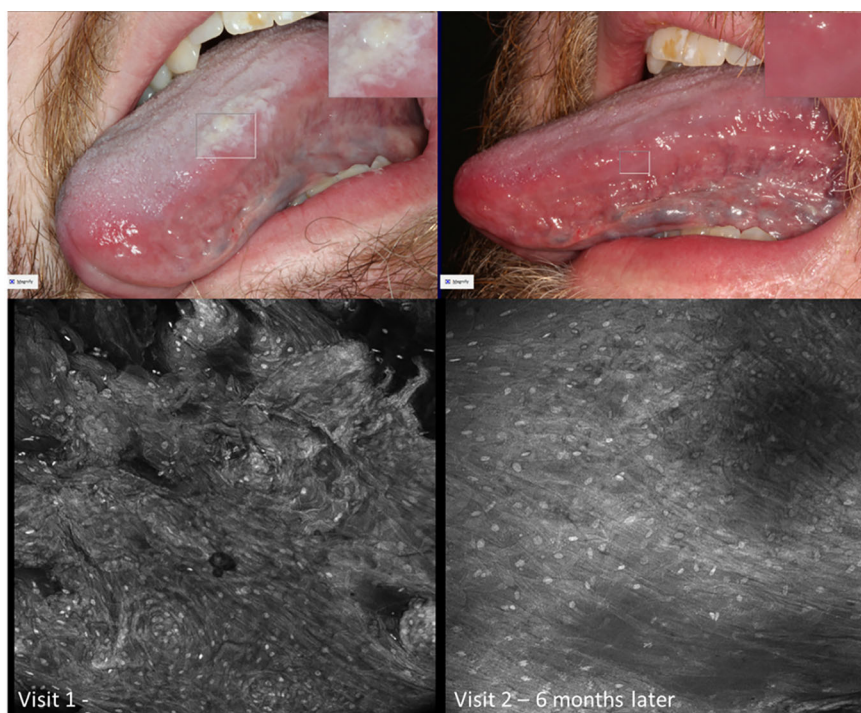


**FIGURE 13**  
 Micrographs of hyperkeratosis and hyperplasia observed with 0.1% fluorescein immediately before scalpel biopsy (performed at Visit 1) and corresponding macrograph photographs. Micrographs demonstrate consistent nuclei size and regular cellular outlines. The lesion resolved 6 months later showing clinically normal lateral tongue mucosa.

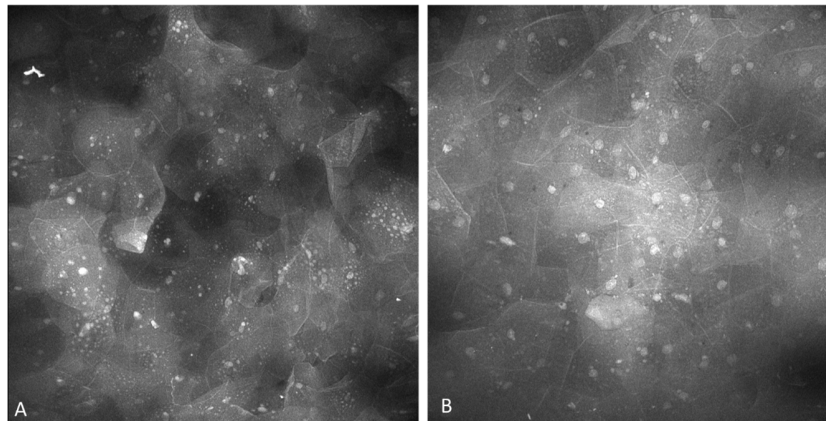


FIGURE 14

Perinuclear granules observed in lesions showing oral lichenoid inflammation, observed with both (A) topical 0.1% fluorescein and (B) topical 0.1% acriflavine.

different parts of the spectrum to enable both pancytoarchitectural visualisation of tissue structure and selective molecular targeted labelling of specific tissue features. Further categorical qualitative and quantitative analysis is required to definitively determine the strength in clinical information the 3 studied agents present. Further, the simultaneous application of acriflavine and fluorescein may be useful to explore.

Unlike physical pathology slides, digital biopsy images have very real potential for rapid comparison over time. Alongside the development of optimizing the digital biopsy image acquisition process, it is also crucial to have an annotation framework such as MouthMap™ which allows for easy annotation and reference to its corresponding intraoral location. In this way, digital health translation can bridge the laboratory to clinic spheres to improve and expedite chair side decision making.

This protocol offers real-time confocal microscopic imaging during oral mucosal assessment. Independent pattern recognition, qualitative as well as quantitative categorical assessments should be developed on captured image features. This should be in addition to focusing on visualizing features expected in traditional histopathology for the thorough assessment of oral mucosal abnormalities. Thereby, consensus based confocal based diagnostic criteria must be further developed and may be based on the consortium of previous confocal work in the field (10, 11)

There is also a need to establish imaging protocols as standard care so that acquisition and archiving of the device-captured images can be applied usefully in the clinical workflow. Digital capture obviously highlights the potential of augmentation for the application of machine learning and artificial intelligence. Although images captured by confocal microscopes have been candidates for deep learning (33), AI has yet to be applied to scanned fibre endoscopic *in vivo* captured images (32). In the future, these require further developments and a translation process back to chairside devices with the makings of a user-friendly

workflow. These are the required steps to develop oral digital biopsies to be a crucial player in delivering the standard of care. As with any new technology, the practical clinical gains must be significant to justify any additional cost, training requirements and changes to workflow.

## 5 Conclusion

This study has demonstrated potential to increase diagnostic precision, augmenting current standard of care, by completing a more comprehensive imaging digital biopsy protocol of the patient without requiring more invasive scalpel biopsies. We have demonstrated successful implemented acquisition and annotation elements. In this way, the need for multiple biopsies may be reduced with onward facilitation of longitudinal comparison. High resolution microscopy of the oral cavity is demonstrated here with the clear capture of micrographic images of quality for pathological assessment of the oral cavity. We predict that the use of non-invasive high-resolution microscopy will have significant utility for the monitoring of oral potential malignant disorders, achieving not only the reduction in the need for scalpel biopsy whilst further allowing for increased data acquisition in less time, thus leading to higher diagnostic precision. This will result in a significant shift in the current paradigm of the visual and pathology-based assessment of individuals living with oral lesions and advance our ability to achieve earliest diagnosis, prevention and diminish mortality from oral cancer.

## Data availability statement

The original contributions presented in the study are included in the article/supplementary materials. Further inquiries can be

directed to the corresponding author.

## Ethics statement

The studies involving human participants were reviewed and approved by University of Melbourne Medicine and Dentistry Human Ethics Sub-Committee (ID 1955205). The patients/participants provided their written informed consent to participate in this study.

## Author contributions

TY, LB and MM contributed to conception and design of the study. PD, TR and LB provided crucial study components for data capture. RR and CM provided organisation of the data capture. Data was acquired by IT, NB and TY. TY wrote the first draft of the manuscript. All authors contributed to manuscript revision, read, and approved the submitted version.

## Funding

A Medical Research Future Fund Award through the BioMedTech Horizons Program 2020 and administered by MTPConnect was awarded to Optiscan Imaging and the Melbourne Dental School. A Dean's Innovation Grant, Faculty of Medicine, Dentistry and Health Sciences, the University of Melbourne awarded to TY in 2020 as a seed grant to commission the MouthMap software in a collaboration with MoleMap Australia & New Zealand.

## Acknowledgments

The authors would also like to acknowledge the incredible software engineers at MoleMap Australia and New Zealand especially founder Adrian Bowling and Alastair Sharfe. We would also like to acknowledge Dental Health Services Victoria, particularly Associate Professor Nicole Heaphy and Victorian

## References

1. National Cancer Institute - Surveillance E, and End Results Program. *Cancer stat facts: oral cavity and pharynx cancer* (2022). Available at: <https://seercancer.gov/statfacts/html/oralcavhtml> (Accessed 4th April 2023).
2. Kaur J, Matta A, Kak I, Srivastava G, Assi J, Leong I, et al. S100A7 overexpression is a predictive marker for high risk of malignant transformation in oral dysplasia. *Int J Cancer* (2014) 134(6):1379–88. doi: 10.1002/ijc.28473
3. Mello FW, Miguel AFP, Dutra KL, Porporatti AL, Warnakulasuriya S, Guerra ENS, et al. Prevalence of oral potentially malignant disorders: a systematic review and meta-analysis. *J Oral Pathol Med* (2018) 47(7):633–40. doi: 10.1111/jop.12726
4. Hsue SS, Wang WC, Chen CH, Lin CC, Chen YK, Lin LM. Malignant transformation in 1458 patients with potentially malignant oral mucosal disorders: a follow-up study based in a Taiwanese hospital. *J Oral Pathol Med* (2007) 36(1):25–9. doi: 10.1111/j.1600-0714.2006.00491.x
5. Wang YY, Tail YH, Wang WC, Chen CY, Kao YH, Chen YK, et al. Malignant transformation in 5071 southern Taiwanese patients with potentially malignant oral mucosal disorders. *BMC Oral Health* (2014) 14:99. doi: 10.1186/1472-6831-14-99
6. Ho P-S, Wang W-C, Huang Y-T, Yang Y-H. Finding an oral potentially malignant disorder in screening program is related to early diagnosis of oral cavity cancer – experience from real world evidence. *Oral Oncol* (2019) 89:107–14. doi: 10.1016/j.oraloncology.2018.12.007
7. Peterson G, Zaroni DK, Ardigo M, Migliacci JC, Patel SG, Rajadhyaksha M. Feasibility of a video-mosaicking approach to extend the field-of-View for reflectance confocal microscopy in the oral cavity *In vivo*. *Lasers Surg Med* (2019). 51(5):439–51 doi: 10.1002/lsm.23090
8. Elliott AD. Confocal microscopy: principles and modern practices. *Curr Protoc cytometry* (2020) 92(1):e68. doi: 10.1002/cpcy.68

Comprehensive Cancer Centre Alliance Head and Neck teams particularly Mr Stephen Kleid, Mr Adrian DeAngelis and lead, Professor David Wiesenfeld.

## Conflict of interest

LB is an employee and shareholder of Optiscan Imaging. TR is a shareholder of Summit Biomedical Imaging, LLC. S.K., S.P. and co-inventor on filed U.S. patent WO2016164771 that covers methods of use for PARPi-FL. TR is also a co-inventor on U.S. patent WO2012074840, covering the composition of matter for PARPi-FL. TR is a paid consultant for Theragnostics, Inc. This arrangement has been reviewed and approved by Memorial Sloan Kettering Cancer Center in accordance with its conflict of interest policies. TY was awarded a Dean's Innovation Grant by the University of Melbourne to commission the MouthMap™ project software in collaboration with MoleMap.

The remaining authors declare that the research was conducted in the absence of any commercial or financial relationships that could be construed as a potential conflict of interest.

The authors declare that this study received funding from The Australian Government awarded through the Medical Research Future Fund to Optiscan Imaging and the University of Melbourne Dental School in collaborative clinical research to improve screening and early diagnosis of oral cancer. This project was funded in 2020 through the BioMedTech Horizons Program and administered by MTPConnect. TY is the lead researcher in this collaboration. The funder was not involved in the study design, collection, analysis, interpretation of data, the writing of this article or the decision to submit it for publication.

## Publisher's note

All claims expressed in this article are solely those of the authors and do not necessarily represent those of their affiliated organizations, or those of the publisher, the editors and the reviewers. Any product that may be evaluated in this article, or claim that may be made by its manufacturer, is not guaranteed or endorsed by the publisher.

9. Nwaneshiudu A, Kuschal C, Sakamoto FH, Anderson RR, Schwarzenberger K, Young RC. Introduction to confocal microscopy. *J Invest Dermatol* (2012) 132(12):e3. doi: 10.1038/jid.2012.429
10. Contaldo M, Lauritano D, Carinci F, Romano A, Di Stasio D, Lajolo C, et al. Intraoral confocal microscopy of suspicious oral lesions: a prospective case series. *Int J Dermatol* (2020) 59(1):82–90. doi: 10.1111/ijd.14574
11. Contaldo M, Di Stasio D, Petrucci M, Serpico R, Lucchese A. *In vivo* reflectance confocal microscopy of oral lichen planus. *Int J Dermatol* (2019) 58(8):940–5. doi: 10.1111/ijd.14410
12. Rangrez M, Bussau L, Ifrit K, Delaney P. Fluorescence *In vivo* endomicroscopy: high-resolution, 3-dimensional confocal laser endomicroscopy (Part 1). *Microscopy Today* (2021) 29(2):32–7. doi: 10.1017/S155192952100050X
13. Canto MI, Anandasabapathy S, Brugge W, Falk GW, Dunbar KB, Zhang Z, et al. *In vivo* endomicroscopy improves detection of Barrett's esophagus-related neoplasia: a multicenter international randomized controlled trial (with video). *Gastrointestinal endoscopy* (2014) 79(2):211–21. doi: 10.1016/j.gie.2013.09.020
14. Thong PS, Tandjung SS, Movania MM, Chiew WM, Olivo M, Bhuvaneshwari R, et al. Toward real-time virtual biopsy of oral lesions using confocal laser endomicroscopy interfaced with embedded computing. *J Biomed Optics* (2012) 17(5):056009. doi: 10.1117/1.JBO.17.5.056009
15. Tan J, Quinn MA, Pyman JM, Delaney PM, McLaren WJ. Detection of cervical intraepithelial neoplasia *in vivo* using confocal endomicroscopy. *BJOG: an Int J Obstetrics Gynaecol* (2009) 116(12):1663–70. doi: 10.1111/j.1471-0528.2009.02261.x
16. Hurlstone DP, Baraza W, Brown S, Thomson M, Tiffin N, Cross SS. *In vivo* real-time confocal laser scanning endomicroscopic colonoscopy for the detection and characterization of colorectal neoplasia. *Br J Surgery* (2008) 95(5):636–45. doi: 10.1002/bjs.5988
17. Abramov I, Park MT, Belykh E, Dru AB, Xu Y, Gooldy TC, et al. Intraoperative confocal laser endomicroscopy: prospective *in vivo* feasibility study of a clinical-grade system for brain tumors. *J neurosurgery* (2023) 138(3):587–97. doi: 10.3171/2022.5.JNS2282
18. Farah CS, Janik M, Woo SB, Grew J, Slim Z, Fox SA. Dynamic real-time optical microscopy of oral mucosal lesions using confocal laser endomicroscopy. *J Oral Pathol Med* (2023). doi: 10.1111/jop.13437
19. Haxel BR, Goetz M, Kiesslich R, Gosepath J. Confocal endomicroscopy: a novel application for imaging of oral and oropharyngeal mucosa in human. *Eur Arch Oto-Rhino-Laryngol* (2010) 267(3):443–8. doi: 10.1007/s00405-009-1035-3
20. Polglase AL, McLaren WJ, Skinner SA, Kiesslich R, Neurath MF, Delaney PM. A fluorescence confocal endomicroscope for *in vivo* microscopy of the upper- and the lower-GI tract. *Gastrointestinal endoscopy* (2005) 62(5):686–95. doi: 10.1016/j.gie.2005.05.021
21. Kiesslich R, Burg J, Vieth M, Gnaendiger J, Enders M, Delaney P, et al. Confocal laser endoscopy for diagnosing intraepithelial neoplasias and colorectal cancer *in vivo*. *Gastroenterology* (2004) 127(3):706–13. doi: 10.1053/j.gastro.2004.06.050
22. Contaldo M, Poh CF, Guillaud M, Lucchese A, Rullo R, Lam S, et al. Oral mucosa optical biopsy by a novel handheld fluorescent confocal microscope specifically developed: technologic improvements and future prospects. *Oral Surg Oral Med Oral Pathol Oral Radiol* (2013) 116(6):752–8. doi: 10.1016/j.oooo.2013.09.006
23. Rouleau M, Patel A, Hendzel MJ, Kaufmann SH, Poirier GG. PARP inhibition: PARP1 and beyond. *Nat Rev Cancer* (2010) 10(4):293–301. doi: 10.1038/nrc2812
24. Reiner T, Lacy J, Keliher EJ, Yang KS, Ullal A, Kohler RH, et al. Imaging therapeutic PARP inhibition *in vivo* through bioorthogonally developed companion imaging agents. *Neoplasia* (2012) 14(3):169–77. doi: 10.1593/neo.12414
25. Kossatz S, Pirovano G, Demétrio De Souza França P, et al. Validation of the use of a fluorescent PARP1 inhibitor for the detection of oral, oropharyngeal and oesophageal epithelial cancers. *Nat Biomed Eng* (2020) 4(3):272–85. doi:10.1038/s41551-020-0526-9
26. Demétrio de Souza França P, Kossatz S, Brand C, Karassawa Zanoni D, Roberts S, Guru N, et al. A phase I study of a PARP1-targeted topical fluorophore for the detection of oral cancer. *Eur J Nucl Med Mol imaging* (2021) 48(11):3618–30. doi: 10.1007/s00259-021-05372-6
27. Kossatz S, Pirovano G, Demétrio De Souza França P, Strome AL, Sunny SP, Zanoni DK, et al. Validation of the use of a fluorescent PARP1 inhibitor for the detection of oral, oropharyngeal and oesophageal epithelial cancers. *Nat Biomed engineering* (2020) 4(3):272–85. doi: 10.1038/s41551-020-0526-9
28. Rangrez M, Bussau L, Ifrit K, Preul MC, Delaney P. Fluorescence *In vivo* endomicroscopy part 2: applications of high-resolution, 3-dimensional confocal laser endomicroscopy. *Microscopy Today* (2021) 29(3):14–26. doi: 10.1017/S1551929521000729
29. Harris PA, Taylor R, Thielke R, Payne J, Gonzalez N, Conde JG. Research electronic data capture (REDCap)—a metadata-driven methodology and workflow process for providing translational research informatics support. *J Biomed informatics* (2009) 42(2):377–81. doi: 10.1016/j.jbi.2008.08.010
30. Harris PA, Taylor R, Minor BL, Elliott V, Fernandez M, O'Neal L, et al. The REDCap consortium: building an international community of software platform partners. *J Biomed informatics* (2019) 95:103208. doi: 10.1016/j.jbi.2019.103208
31. Contaldo M, Agozzino M, Moscarella E, Esposito S, Serpico R, Ardigò M. *In vivo* characterization of healthy oral mucosa by reflectance confocal microscopy: a translational research for optical biopsy. *Ultrastructural pathol* (2013) 37(2):151–8. doi: 10.3109/01913123.2013.776656
32. Ramani RS, Tan I, Bussau L, Angel CM, McCullough M, Yap T. Confocal microscopy in oral cancer and oral potentially malignant disorders: a systematic review. *Oral Dis* (2022). doi: 10.1111/odi.14291
33. von Chamier L, Laine RF, Jukkala J, Spahn C, Krentzel D, Nehme E, et al. Democratizing deep learning for microscopy with ZeroCostDL4Mic. *Nat Commun* (2021) 12(1):2276. doi: 10.1038/s41467-021-22518-0